Technical Report

TR-12-13

A Study of Consequences of Freezing of Concrete Structures for Storage of Nuclear Waste due to Permafrost

Tang Luping
Division of Building Technology
Chalmers University of Technology

Dirch H. Bager
DHB-Consult

April 2013

Svensk Kärnbränslehantering AB
Swedish Nuclear Fuel
and Waste Management Co

Box 250, SE-101 24 Stockholm
Phone +46 8 459 84 00

ISSN 1404-0344
SKB TR-12-13
ID 1318304

A Study of Consequences of Freezing of Concrete Structures for Storage of Nuclear Waste due to Permafrost

Tang Luping
Division of Building Technology
Chalmers University of Technology

Dirch H. Bager
DHB-Consult

April 2013

Keywords: Cement paste, Concrete, Freezing, Nuclear waste, Permafrost.

Abstract

This report presents the results from a study of consequences of freezing of concrete structures for storage of nuclear waste due to the action of permafrost. The experimental data measured from over 20 years aged cement paste specimens were used as input parameters of freezable water and mechanical properties. The model based on the poroelasticity was employed for calculation of overpressure of unfrozen liquid and strain of the porous body. The calculation results show that micro-cracking may occur due to ice formation in the fully water-saturated hardened cement pastes under the action of permafrost. The main consequences of this ice formation induced micro-cracking after one cycle of freezing-thawing at temperature –5°C and –10°C will be as follows:

- The compressive strength of the silo concrete may in a normal case be reduced by 1% and 2%, respectively, and in the worst case by 15%, and the compressive strength of the 1 BMA concrete may in a normal case be reduced by 1% and 4%, respectively, and in the worst case by 19%.
- The tensile strength of the silo concrete may in a normal case be reduced by 11% and 17%, respectively, and in the worst case by 45%, and the tensile strength of the 1 BMA concrete may in a normal case be reduced by 13% and 22%, respectively, and in the worst case by 51%.
- The hydraulic conductivity of both the silo and the 1 BMA concrete may in a normal case be increased by not more than 2%, and in the worst case by not more than 10%.
- It is hardly possible to lead a structural collapse due to the reduction in tensile strength in both the silo and the 1 BMA concrete containers filled inside with grout after filling of nuclear waste, unless the steel reinforcement in the reinforced concrete structure is designed with significantly less amount of steel bars and there exists large unfilled volume under the concrete roof.

Contents

1 Background

In SKB's (Swedish Nuclear Fuel and Waste Management Co.) report R-07-60 (Emborg et al. 2007), it was concluded that the concrete silo in SFR 1 (the Final Repository for short-lived low- and intermediate-level Radioactive waste) will be completely destructed under the permafrost period when temperature decreases to –5°C and –10°C. This conclusion was based on simple assumptions that the unfrozen water is absolutely uncompressible and the volume increase (9% under an unconfined condition) when freezable water becomes ice will be fully contributed to the volumetric dilation of concrete. With these assumptions, the minimum frozen water of 5 l/m^3 will result in a linear expansion of concrete by 0.15‰, which is the critical value for tensile damage of concrete. In R-07-60 (Emborg et al. 2007), the freezable water in the concrete was estimated to be 17 and 30 l/m^3 at –5°C and –10°C, respectively, which is significantly larger than the minimum frozen water (5 l/m^3) for damage of concrete, leading to the above conclusion. Report R-07-60 (Emborg et al. 2007) does not give the information about at which temperature the first cracking can occur. On the request of SKB, we carried out this study to further investigate the consequence of freezing of concrete structures due to permafrost action.

2 Prerequisites and limitations

This study will be limited to two concrete structures in SFR 1:

- Concrete silo surrounded by a bentonite clay buffer.
- Concrete 1 BMA (a rock vault structure) surrounded by gravel fillers.

2.1 Properties of concrete

The properties of concrete used in SFR 1 are summarised in Table 2-1.

It is assumed that the waste containers in both the concrete silo and 1 BMA are surrounded by cementitious mortar (as grout) with *w/c* (water-cement ratio) of about 1.1 (implying earlier freezing of pore water in the grout than that in the concrete structures). It is also assumed that, after long-term exposure, the concrete structures are fully saturated by the ground water.

2.2 Cracking criterion

In Emborg et al. (2007), the criterion of volumetric strain, $\varepsilon_F = 0.45‰$, was used as the limit for fracture. According to Bager (2010), both tensile splitting strength and dynamic modulus of concrete cured in the water decreased after 25 years. It was found from his investigation that, as an average from the measurements of 16 types of concrete, tensile splitting strength decreased by about 30% (implying a reduction factor 0.7) and dynamic elastic modulus decreased by about 20% (implying a reduction factor 0.8) after 25 years when compared with the data measured after 5–10 years. Therefore, it is more realistic to take the value $\varepsilon_F = 0.40‰$ (as a result of $0.7/0.8\times0.45‰$) for aged concrete as cracking criterion.

The other parameters to be used in the calculation include:

- Elastic modulus $E_c = 0.8\times E_{EC2} = 0.8\times 10\, f_{cu}^{0.31}$ GPa (where E_{EC2} is the modulus according to EC 2, SS-EN 1992-1-1:2005, and 0.8 is a reduction factor for the aged concrete)
- Poisson's ratio $v_p = 0.2$ (according to SS-EN 1992-1-1:2005).

Table 2-1. Properties of concrete used in SFR 1 in Forsmark.

Properties	Silo[1)]	1 BMA[2)]
Cement type	Swedish structural cement (CEM I 42.5 SR/MH/LA)	
Water-cement ratio *w/c*	0.47 ± 0.03	0.62 ± 0.07
Compresive strength f_{cu}, MPa	48 ± 5	40 ± 5
Cement content, kg/m^3	350	300
Aggregate volume fraction[3)]	0.7	
Aggregate elastic modulus[4)], GPa	50	

1) Based on Emborg et al. (2007) but with symmetrical deviation of 48 ± 5 MPa in compressive strength instead of 43–58 MPa with mean 48 MPa.
2) Estimated based on the previous Swedish concrete class K30.
3) Estimated based on general design of concrete mix proportion, which is in agreement with Höglund (2001) for the concrete silo.
4) Assumed for granitic aggregate.

2.3 Freezing condition

According to Näslund (2006) the temperature gradient (Table 3-8 on page 98) under the ground in Forsmark is 0.011°C/m (11°C/km) and the rate of propagation of permafrost front (Figure 3-42 on page 101) will be less than 8 cm/year, assuming the surface temperature –20°C after 2000 years. This means that the cooling rate is very slow. The ground water surrounding the bentonite clay layer and concrete silo or the layer of gravel fillers surrounding the concrete 1 BMA will be frozen prior to the ice formation in the concrete. Therefore, the ice formation in both the concrete structures is under the undrained condition.

3 Depression of freezing point in micro porous materials

3.1 Effect of pore size

The freezing point of evaporable water in micro porous materials depends on the pore size. The smaller pore size – the lower the freezing temperature, see Figure 3-1 from Sellevold and Bager (1980).

3.2 Effect of salinity

Salts in the pore solution leads to freezing point depression of the solution. The freezing point depression can be calculated as:

$$\Delta T = K_F \cdot \frac{nC}{M(100 - C)} \tag{3-1}$$

where

K_F = the cryoscopic constant, K_F = 1,860 K×g/mol.

n = Number of ions per individual molecule of solute, e.g. n = 2 for NaCl.

M = Mole weight, g/mol.

C = weight percentage of salt/(salt + water).

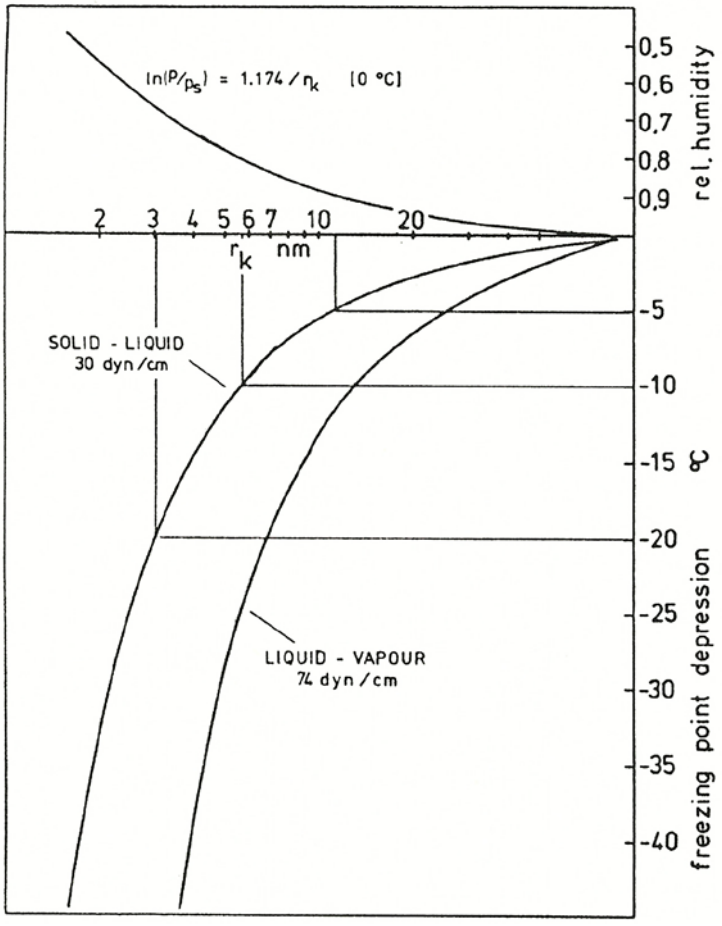

Figure 3-1. *Freezing point depression as a function of pore size (calculated as cylindrical pores). If the pores are fully saturated, the freezing point depression follows the "solid-liquid line", while the freezing point in partly saturated specimens follows the "liquid-vapour line". [30 dyn/cm and 74 dyn/cm are the surface tension of the ice-water and water-vapour interfaces, respectively], according to Sellevold and Bager (1980).*

For the actual storage area in Forsmark and Laxemar, Näslund (2006) has given the information about the salt content in the groundwater, see Figure 3-2.

The concentrations at 50–60 m depths in Forsmark and 500 m depths in Laxemar are given in Table 3-1.

In normal freeze-thaw measurements, super-cooling during the freezing of the pore solution normally takes place. Hence, the freezing point cannot be judged from cooling experiments, but only from the measurements during heating. Figure 3-3 shows apparent heat capacity (an indication of ice-melting) during heating for saturated hardened cement paste specimens with w/c ratios of 0.40 and 0.60, containing NaCl-solutions of 0, 2.5, 5, 10 and 20 mass%.

From Figure 3-3 it can be seen that the NaCl concentration shall be above approximately 15% in order to lower the freezing point to below –10°C. The freezing point depression for solutions in small pores do not follow the normal rules for freezing of salt solutions, since the mobility of the salt ions are so limited, that they will be incorporated in the formed ice rather than being pushed out and up concentrating the unfrozen part of the liquid until freezing at the eutectic temperature.

From Table 3-1 it can be seen, that the concentration of salts (NaCl, $CaCl_2$, $CaSO_4$, etc) is far below 1%, so irrespective of the number of ions in the solution, the freezing point depression in the ground water is negligible, and therefore of no influence for freezing in the concrete containers, when temperatures reach –5 or –10°C. Thus freezing of the pore water will be like freezing of normal pore water, starting with freezing point close to 0°C, see Figure 3-3.

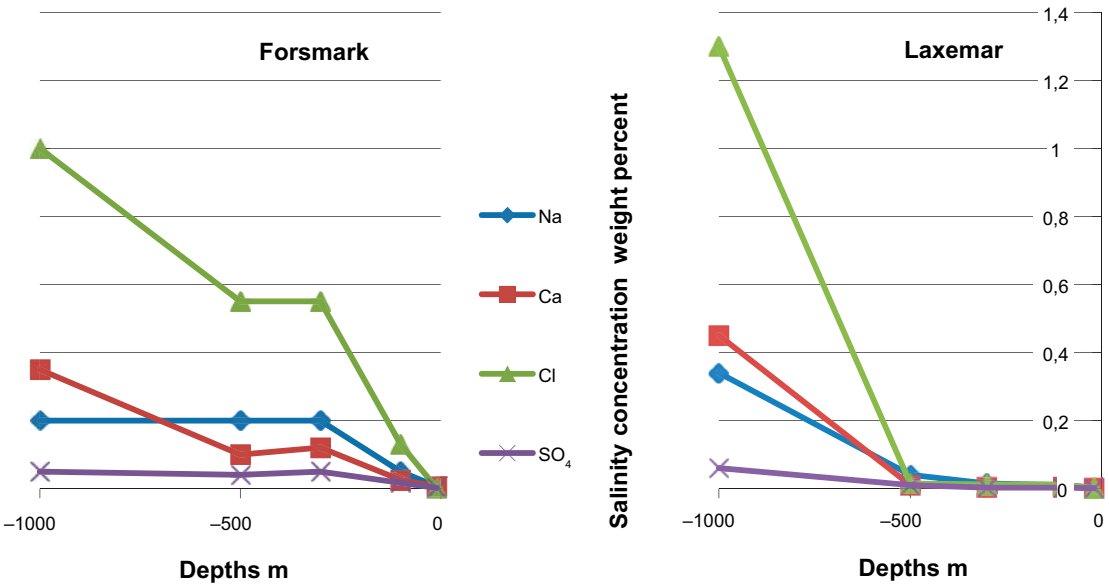

Figure 3-2. *Salinity in the groundwater in Forsmark & Laxemar (Näslund 2006). For the storage of the nuclear waste in Forsmark the depth between 50 and 60 m is relevant. For the storage about –500 m in Laxemar, 500 m is relevant.*

Table 3-1. Concentrations of Na, Ca, Cl & SO_4 in 50–60 m depth under Forsmark and 500 m under Laxemar (Näslund 2006).

	Forsmark	Laxemar
	Concentration kg/kg	
Na	0.00030	0.00040
Ca	0.00015	0.00010
Cl	0.00065	0.00015
SO_4	0.00010	0.00010

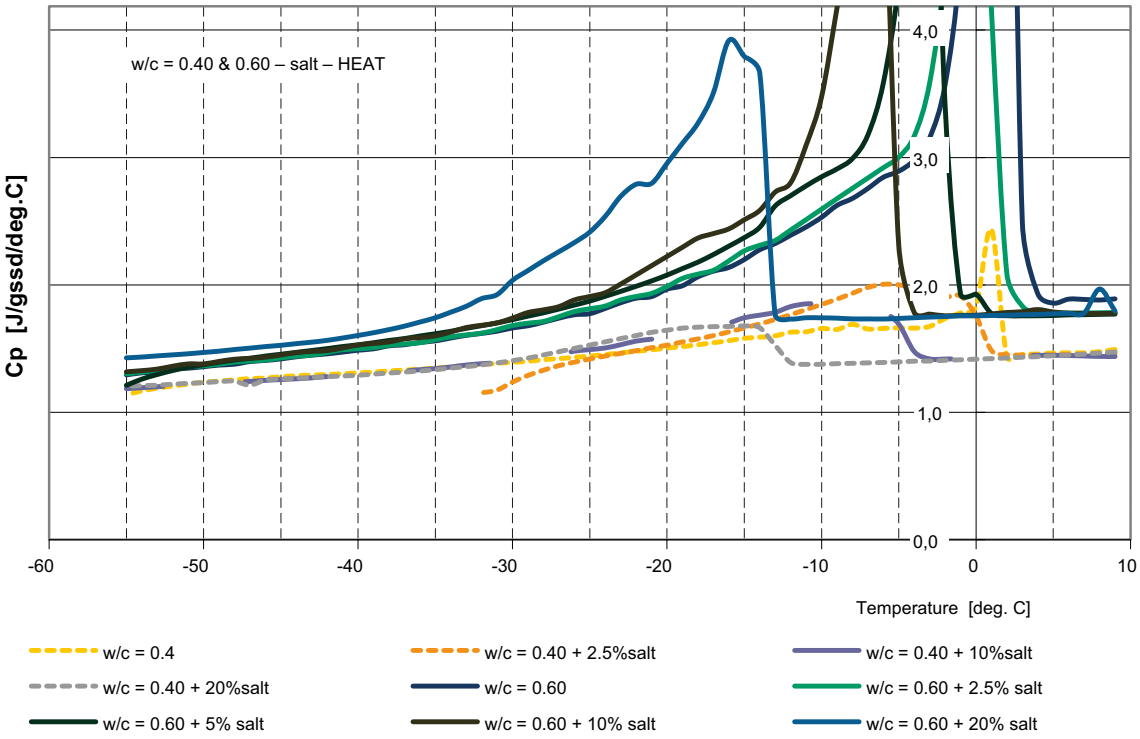

Figure 3-3. *Freezing point depression of NaCl-solutions in hardened cement paste specimens. [based on the experimental data from Bager, gssd = weight in gram per saturated surface dry sample].*

Vidstrand and Rhen (2011) informed that the salinity in the surrounding of the silos can increase up to 2% during the permafrost passage. In the bentonite layer, having a larger porosity compared to the concrete and cement paste, this may result in a situation, where ice is formed, and water with increasing salinity will be present. The salinity in the water will be controlled by the temperature; increasing up to approximately 15% with decreasing temperature down to –10°C. If this salt water is in contact with the silo concrete surface, then osmosis can lead to water movement from the concrete to the salt water, so more ice can be formed outside the concrete. Salts might also migrate into the concrete, and thereby lower the freezing point in the capillary pore water, as illustrated in Figure 3-3. Increased salinity in the surface layer and in the surroundings can lead to attraction of water from the concrete layer below the surface, resulting in a decrease in the degree of water saturation in concrete. Because the period of increase in salinity during the permafrost passage is relative short when compared with the period of permafrost, this temporary effect will not be taken into account in the calculation of the stress and strain during freezing.

4 Freezable water

Owing to different pore sizes in concrete, the amount of freezable water varies with temperature. The Differential Scanning Calorimeter is usually used to measure the ice formation from which the amount of freezable water can be calculated. Bager and Hansen (1999) reported their test results from the cement paste samples with *w/c* 0.50 cured in lime water for 1 and 22 years, as shown in Figure 4-1. This is perhaps the unique data available for the aged cement paste. The increase in ice formation during the 21 years storage can be explained by the formation of C_3AS_6 or C_3AS_3 which are stable crystalline forms of calcium aluminate hydrates or silicates. These have a higher density than ettringite, crystalline monosulphate and carbonate, which no longer exists in the pastes. It can be seen from Figure 4-1 that the freezable water in the range of 0 and –10°C is proportional to the decrease of temperature. Jacobsen et al. (2004) proposed an equation for calculation of the amount of freezable water w_{fT}, which is assumed proportional to the evaporable water content in the concrete, that is,

$$w_{f\,T} = -\beta w_e (T_M - T) = -\beta w_e \Delta T \qquad (4\text{-}1)$$

where

β = Proportional factor,

w_e = Evaporable water content in concrete,

T_M = The melting point of ice, T_M = 0°C or 273 K under the standard condition, and

ΔT = Undercooling temperature, $\Delta T = (T_M - T)$.

The curves in Figure 4-1 illustrate that the relationship between ice formation and evaporable water content is not linear. Hence Equation 4-1 should be limited to a small temperature range, for example, between 0°C and –10°C. In the experiments reported by Bager and Hansen (1999), the measured evaporable water content in the samples cured for 1 and 22 years is 311 and 350 mg/g dry paste, respectively. Based on Figure 4-1, the β values are estimated to be 0.004 and 0.020 for the cement paste cured for 1 and 22 years, respectively. Because the concrete for storage of nuclear wastes should be sufficiently old, β = 0.02 will be adopted as a basic value for calculation of stress and strain in this study. For a non-air-entrained concrete with *w/c* 0.47, the evaporable water will be about 130 kg/m^3, including capillary and gel pores in the paste, entrapped air and possible pore spaces in the ITZ (Interfacial Transition Zone), between paste and aggregate This implies a quantity of freezable water of about 13 kg/m^3 at –5°C and 26 kg/m^3 at –10°C. This value is slightly lower than those (17 kg/m^3 at –5°C and 30 kg/m^3 at –10°C) reported in Emborg et al. (2007), which were estimated based on the pore size distribution measured by the mercury intrusion porometry. This method may distort the actual pore structure under the high vacuum treatment prior to the mercury intrusion.

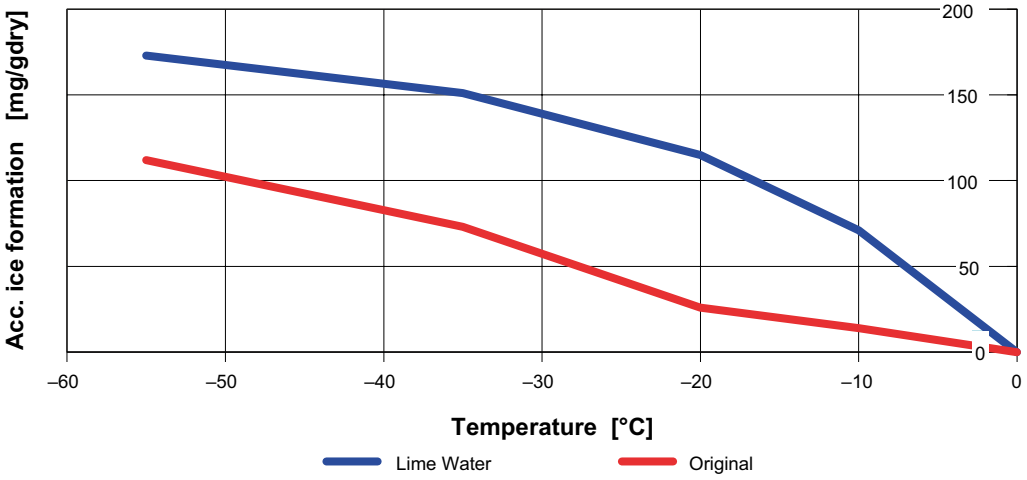

Figure 4-1. *The accumulated ice formation during cooling for two specimens with w/c-ratio of 0.50. Original = Never dried, stored in limewater at 20°C for 1 year. Lime Water = Never dried, stored in limewater at 20°C for 22 years.*

5 Stress and strain during freezing

As mentioned in Section 2.3, the ground water surrounding the bentonite clay layer and concrete silo and the layer of gravel fillers surrounding the concrete structure in 1 BMA will be frozen prior to the ice formation in the concrete. Therefore, the ice formation in both concrete structures is under the undrained condition. Under such a condition, the increased pressure in the unfrozen liquid due to ice formation will not lead to a liquid flow but result in stress and strain in the unfrozen liquid and the surrounding solids (hardened cement paste and aggregates) that confine the unfrozen liquid. In order to calculate the strain in the ice-liquid-solid system, the model based on poroelasticity should be used. Coussy and Monteiro (2009) proposed the following formulas for calculating the overpressure in the unfrozen liquid during freezing:

$$\Delta p_{\mathrm{L}} = p_{\mathrm{L}} - p_{\mathrm{atm}} = \left(p_{\mathrm{L}} - p_{\mathrm{atm}}\right)^{\mathrm{Cryo}} + \left(p_{\mathrm{L}} - p_{\mathrm{atm}}\right)^{\mathrm{Hydrau}} + \left(p_{\mathrm{L}} - p_{\mathrm{atm}}\right)^{\mathrm{Therm}} \tag{5-1}$$

where

$$\left(p_{\mathrm{L}} - p_{\mathrm{atm}}\right)^{\mathrm{Cryo}} = -\frac{AK_{\mathrm{p}}M}{K_{\mathrm{u}}} \cdot \frac{\left(1 + b^2\varphi_{\mathrm{C}}\right)}{M_{\mathrm{C}}} \cdot S_{\mathrm{M}}\Delta T \tag{5-2}$$

$$\left(p_{\mathrm{L}} - p_{\mathrm{atm}}\right)^{\mathrm{Hydrau}} = \frac{AK_{\mathrm{p}}M}{K_{\mathrm{u}}}\left(1 - \frac{\rho_{\mathrm{C}}^{0}}{\rho_{\mathrm{L}}^{0}}\right) \cdot \phi_0\varphi_{\mathrm{C}} \tag{5-3}$$

$$\left(p_{\mathrm{L}} - p_{\mathrm{atm}}\right)^{\mathrm{Therm}} = \frac{3AK_{\mathrm{p}}M}{K_{\mathrm{u}}}\phi_0\left(\alpha_{\mathrm{S}} - \varphi_{\mathrm{C}}\alpha_{\mathrm{C}} - \varphi_{\mathrm{L}}\alpha_{\mathrm{L}}\right) \cdot \Delta T \tag{5-4}$$

where

$$\frac{1}{A} = 1 - \left(1 - \frac{\rho_{\mathrm{C}}^{0}}{\rho_{\mathrm{L}}^{0}}\right) \cdot \frac{K_{\mathrm{p}}M}{K_{\mathrm{u}}} \cdot \left(\frac{1}{M_{\mathrm{C}}} + \frac{b^2\varphi_{\mathrm{C}}}{K_{\mathrm{p}}}\right) \tag{5-5}$$

$$\frac{1}{M} = \frac{b - \phi_0}{K_{\mathrm{S}}} + \phi_0 \cdot \left(\frac{\varphi_{\mathrm{C}}}{K_{\mathrm{C}}} + \frac{\varphi_{\mathrm{L}}}{K_{\mathrm{L}}}\right) \tag{5-6}$$

$$\frac{1}{M_{\mathrm{C}}} = \frac{\left(b - \phi_0\right)\varphi_{\mathrm{C}}}{K_{\mathrm{S}}} + \frac{\phi_0\varphi_{\mathrm{C}}}{K_{\mathrm{C}}} \tag{5-7}$$

$$b = 1 - \frac{K_{\mathrm{p}}}{K_{\mathrm{S}}} \tag{5-8}$$

p_{L}, p_{atm} = Static pressure of unfrozen liquid and atmospheric pressure, respectively,

ρ^0_{C}, ρ^0_{L} = Specific density of ice crystal and liquid at the melting point ($\rho^0_{\mathrm{L}} = 1$ and $\rho^0_{\mathrm{C}} = 0.916$ at $T_{\mathrm{M}} = 0°\mathrm{C}$), respectively,

ϕ_0 =Initial porosity of porous body,

φ_{C} = Degree of ice saturation and at a given undercooling, $\varphi_{\mathrm{C}} \approx w_{\mathrm{fT}}/w_{\mathrm{e}}$,

φ_{L} = Fraction of unfrozen liquid at a given undercooling, $\varphi_{\mathrm{L}} = 1 - \varphi_{\mathrm{C}}$,

S_{M} = Melting entropy of ice,

α_{S}, α_{C}, α_{L} = Thermal expansion coefficient of the solid matrix, ice and liquid, respectively,

K_{C}, K_{L} = Bulk moduli of ice crystal and unfrozen liquid, respectively,

K_{p}, K_{u} = Bulk moduli of porous body when its pores are empty and saturated with fictitious fluid of ice and unfrozen liquid,

K_{s} = Bulk modulus of solid matrix in the porous body, and

b = Biot coefficient of porous body.

In the above equations, the superscript "Cryo" denotes due to micro-cryo-suction, "Hydrau" due to hydraulic pressure and "Therm" due to thermal deformation. The bulk modulus K_u is expressed by the following equation:

$$K_u = K_p + b^2 M \tag{5-9}$$

The bulk modulus K_p can be calculated from the elastic modulus E_p and Poisson's ratio v_p of the porous body, that is,

$$K_p = \frac{E_p}{3(1-2\nu_p)} \tag{5-10}$$

The bulk modulus K_S is related to K_p and porosity ϕ_0, and can be expressed by (Hashin and Shtrikman 1963):

$$K_S = K_p\left(\frac{1+\phi_0}{1-\phi_0}\right) \tag{5-11}$$

The values of $\rho^0_L = 1$ and $\rho^0_C = 0.916$ at $T_M = 0°C$ will be used in the calculation. The values of other parameters used by Coussy and Monteiro (2008) will be adopted in the calculations in this study, that is,

$S_M = 1.2$ MPa/°C at $T_M = 0°C$

$K_L = 1.79$ GPa and $K_C = 7.81$ GPa at –10°C

$\alpha_S = 18\times10^{-6}$/°C, $\alpha_C = 51.7\times10^{-6}$/°C and $\alpha_L = -95.4\times10^{-6}$/°C.

The volumetric strain in the porous body can now be expressed by the following equation:

$$\varepsilon = \left(\frac{1}{K_p} - \frac{1}{K_s}\right)\Delta p_L - 3\alpha_S \Delta T \tag{5-12}$$

Because the degree of ice saturation, φ_C, is dependent on the freezable water according to Equation 4-1, it is obvious that the strain of water in a saturated porous body is a function of undercooling temperature. When the strain during freezing reaches the strain limit for fracture, ε_F, cracking occurs and the stress releases. With the further decrease of temperature, the cycle of new strain starts and the new cracking occurs again when the strain reaches the strain limit for fracture.

6 Basic calculation

The composition and properties of the concrete used in the silo and 1 BMA in SFR 1 have been listed in Table 2-1 in Section 2.1. The volumetric strain of 0.4‰ as described in Section 2.2 is used as a criterion of cracking. Because the hardened cement paste is surrounded by large particles of aggregate, and concrete itself is reinforced by steel bars, these cracks cannot be concentrated but should be relatively homogeneously distributed in the concrete structure. This means that the volumetric strain of 0.4‰, corresponding to a linear strain of about 0.13‰, may result in a crack with the maximum wideness of 0.13 mm per meter of hardened cement paste. It should be noted that the number of cracking in the following calculation does not necessarily mean the actual number of cracks with a wideness of 130 μm but just an indication of equivalent quantity of many micro-cracks with a size in the term of wideness less than 130 μm.

Because the aggregate can be considered as a non-porous body, the calculation will be based on the cement paste in concrete as porous body. Assuming the paste has the same compressive strength as concrete, the elastic modulus of paste, E_p, can be solved from the combined model (cf. Model C in Domone and Illston (2010), that is,

$$\frac{1}{E_c} = \frac{\left(1-\sqrt{g}\right)}{E_p} + \frac{\sqrt{g}}{E_a \cdot g + E_p \cdot \left(1-\sqrt{g}\right)} \tag{6-1}$$

where E_a is the elastic modulus of the aggregate and g is the volume concentration of aggregates. A value of E_a = 50 GPa is assumed for granite aggregates, as shown in Table 2-1.

The porosity of hardened cement paste is calculated based on Power's model, taking the specific density of water $\rho_w = 1$, that is, the total porosity, ϕ_0 is

$$\phi_0 = \frac{w/c - 0.75 W_n^0 \alpha_h}{w/c + \frac{\rho_W}{\rho_C}} \tag{6-2}$$

where w/c is the water-cement ratio, the specific non-evaporable water $W_n^0 = 0.23$ gram per gram of hydrated cement, the specific density of cement $\rho_c = 3.15$, and the degree of hydration $\alpha_h = 1$ (assuming fully hydrated). Under the fully saturated condition, the evaporable water content will be $w_e = \phi_0 \times 1{,}000$ kg per m^3 of cement paste.

The porosity contributed by the gel pores in the hardened cement paste is

$$\phi_{gel} = \frac{\phi_{gel}^0}{1-\phi_{gel}^0} \cdot \frac{\left(\frac{1}{\rho_C} + 0.75 W_n^0\right)\alpha_h}{w/c + \frac{\rho_W}{\rho_C}} \tag{6-3}$$

where ϕ_{gel} is the porosity contributed by the gel pores, which has the porosity $\phi^0_{gel} = 0.28$.

The porosity contributed by the capillary pores in the hardened cement is the difference between the above equations, that is,

$$\phi_{cap} = \frac{w/c - \left(\frac{\frac{\rho_W}{\rho_C} \cdot \phi_{gel}^0 + 0.75 \cdot W_n^0}{1-\phi_{gel}^0}\right)\alpha_h}{w/c + \frac{\rho_W}{\rho_C}} \tag{6-4}$$

Case 1: In this case, we take the mean values of *w/c* = 0.47 and compressive strength f_{cu} = 48 MPa as reference for the silo concrete and *w/c* = 0.62 and compressive strength f_{cu} = 40 MPa as reference for the 1 BMA concrete. The calculated hydraulic pressures and strains with the mean values of *w/c* and strength are shown in Figures 6-1 and 6-2. It can be seen from Figure 6-1 that the hydraulic pressures in the pastes with two different *w/c* values are very similar, that is, the pressure due to micro-cryo-suction is negative but very small, whilst the hydraulic pressure due to density difference is very high. As expected, the thermal deformation results in a positive hydraulic pressure because the water expands while the solid matrix shrinks when temperature decreases. Figure 6-2 shows that the strain will result in the first cracking at –2.0°C in the paste with *w/c* 0.47 (silo concrete) and at –1.5°C in the paste with *w/c* 0.62 (1 BMA concrete). If the temperature decreases to –5°C, there will be 2 times of cracking (resulting in micro-cracks with an increase in pore volume by 2×0.04% = 0.08%) in the silo concrete, and 3 times of cracking (resulting in micro-cracks with an increase in pore volume by 3×0.04% = 0.12%) in the 1 BMA concrete. If the temperature decreases to –10°C, totally 5 times of cracking (resulting in micro-cracks with a total increase in pore volume by 5×0.04 = 0.2%) in the silo concrete, and 7 times of cracking (resulting in micro-cracks with a total increase in pore volume by 7×0.04 = 0.28%) in the 1 BMA concrete.

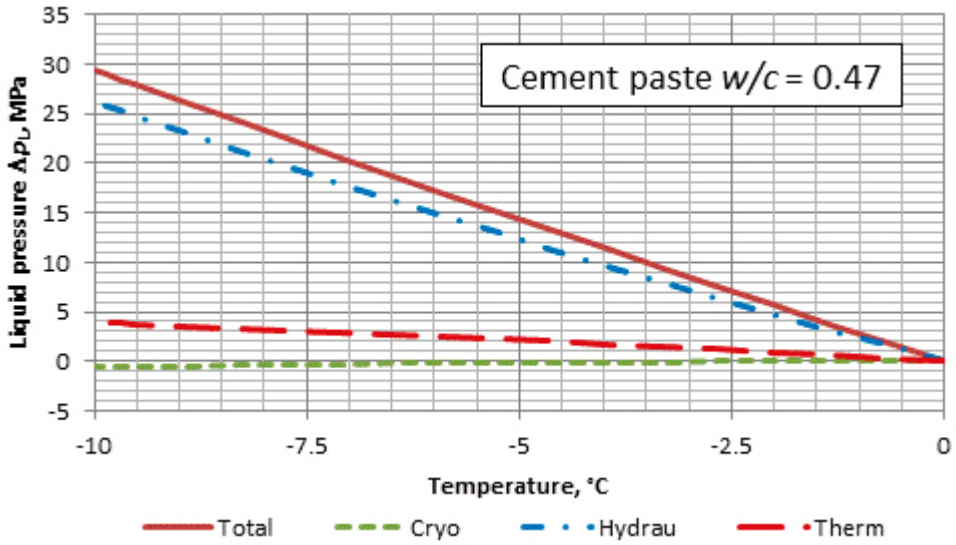

Figure 6-1a. *Calculated liquid pressures in hardened cement paste with w/c 0.47 (the silo concrete).*

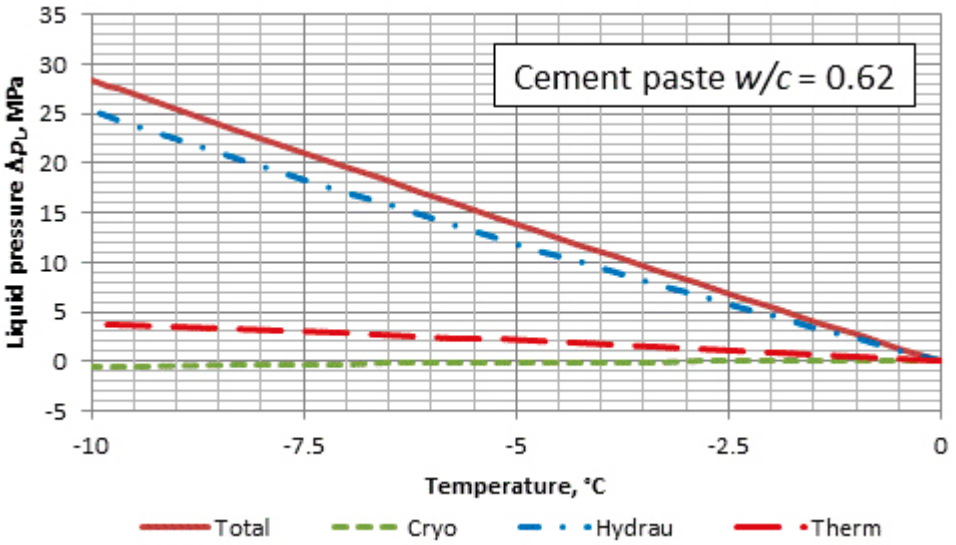

Figure 6-1b. *Calculated liquid pressures in hardened cement paste with w/c 0.62 (the 1 BMA concrete).*

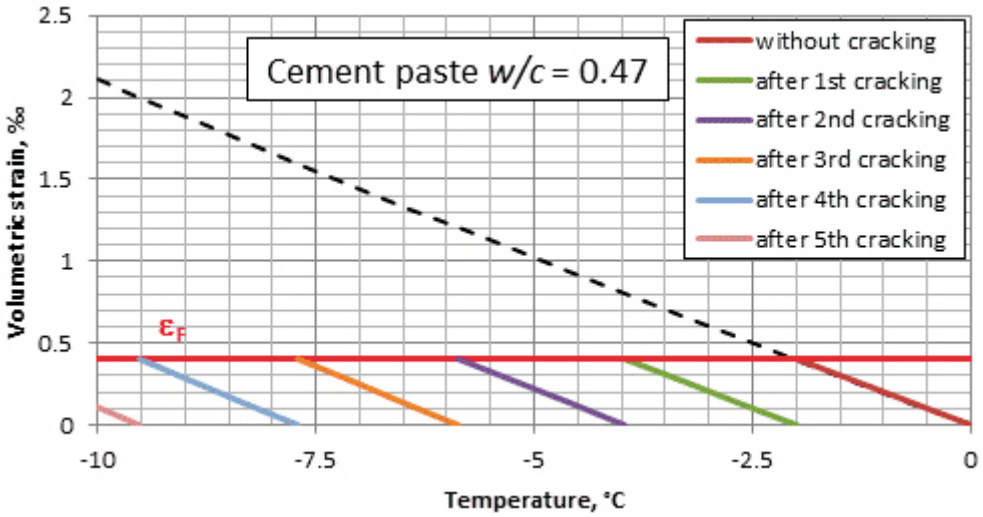

Figure 6-2a. *Volumetric strain and cracking during freezing in hardened cement paste with w/c 0.47 (the silo concrete).*

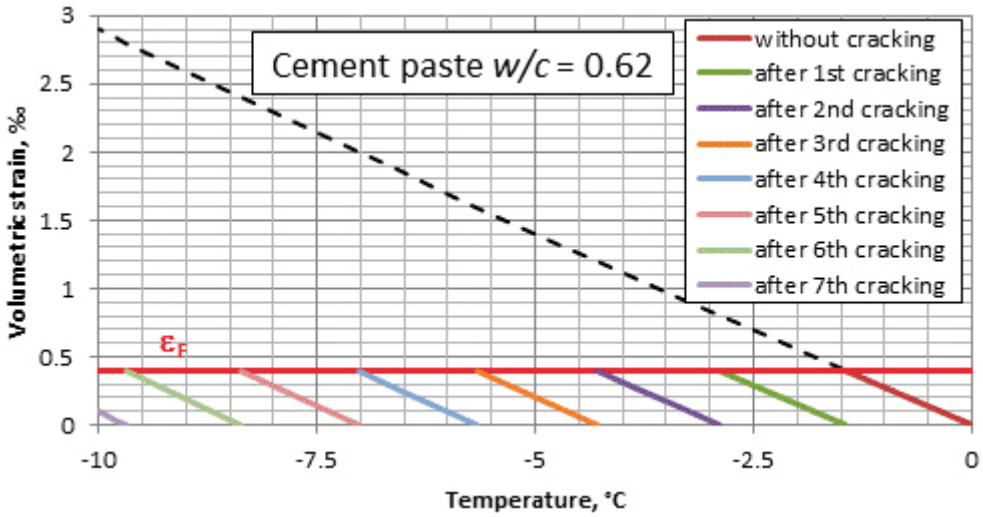

Figure 6-2b. *Volumetric strain and cracking during freezing in hardened cement paste with w/c 0.62 (the 1 BMA concrete).*

To evaluate the uncertainty due to deviation of concrete quality (the uncertainty due to ice formation rate will be discussed in the next section), we take the values of *w/c* = (mean – deviation) and f_{cu} = (mean + deviation) in Table 2-1 as upper limit, and the values of *w/c* = (mean + deviation) and f_{cu} = (mean – deviation) in Table 2-1 as lower limit to calculate the stresses and strains during freezing. The calculated results are shown in Figures 6-3 and 6-4 and summarized in Tables 6-1 and 6-2.

It can be concluded from the calculation results that, in the hardened cement paste of the silo concrete in SFR 1, possible cracking may occur when the temperature decreases to the range of –1.8°C and –2.3°C. It may occur 2 times of cracking if the temperature decreases to –5°C and 4–5 times of cracking if the temperature decreases to –10°C.

In the hardened cement paste of the 1 BMA concrete in SFR 1, possible cracking may occur when the temperature decreases to the range of –1.3°C and –1.7°C. It may occur 3–4 times of cracking if the temperature decreases to –5°C and 6–8 times of cracking if the temperature decreases to –10°C.

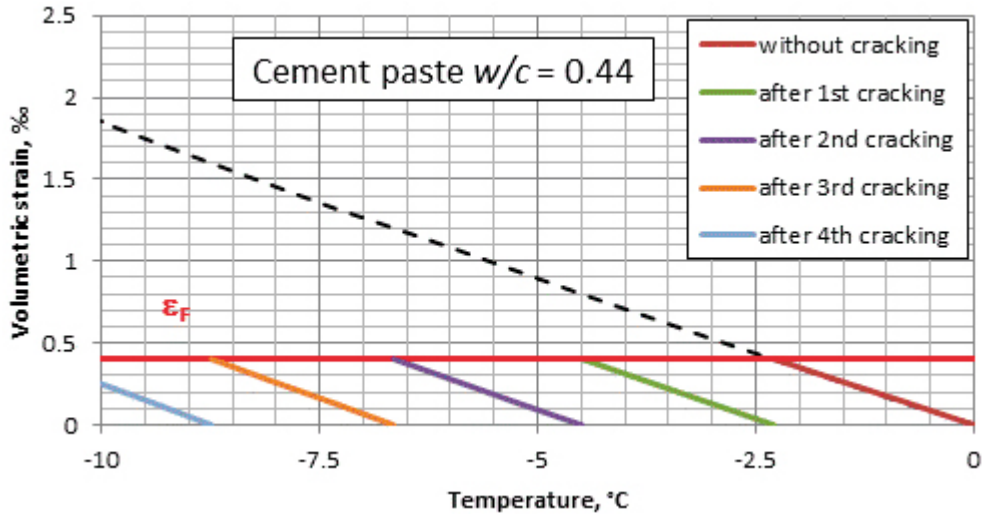

Figure 6-3a. *Possible cracking during freezing in hardened cement paste in the silo concrete with w/c 0.44 (as the upper limit).*

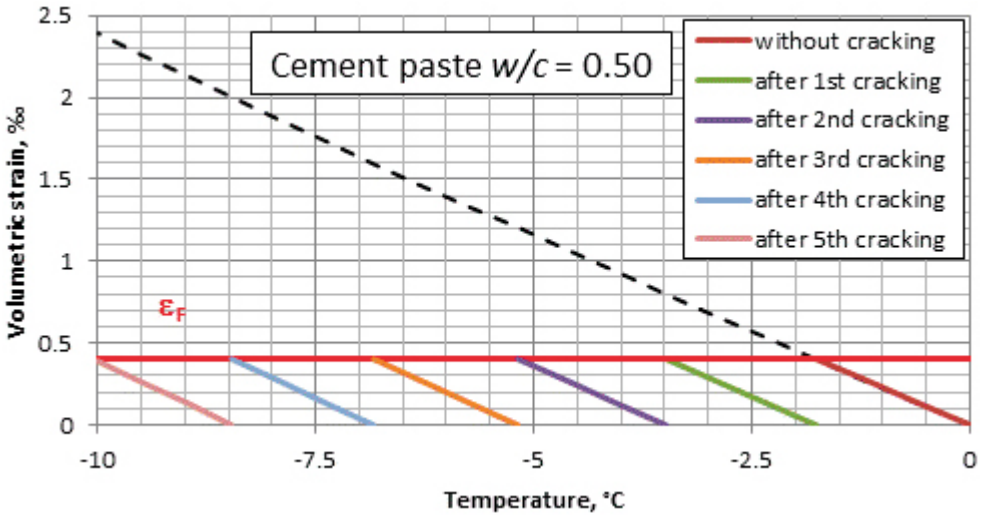

Figure 6-3b. *Possible cracking during freezing in hardened cement paste in the silo concrete with w/c 0.50 (as the lower limit).*

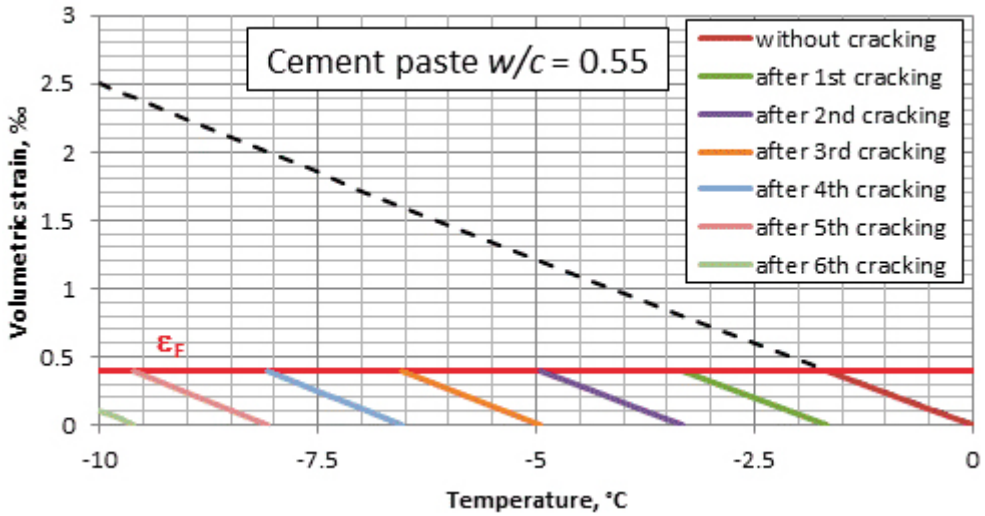

Figure 6-4a. *Possible cracking during freezing in hardened cement paste in the 1 BMA concrete with w/c 0.55 (as the upper limit).*

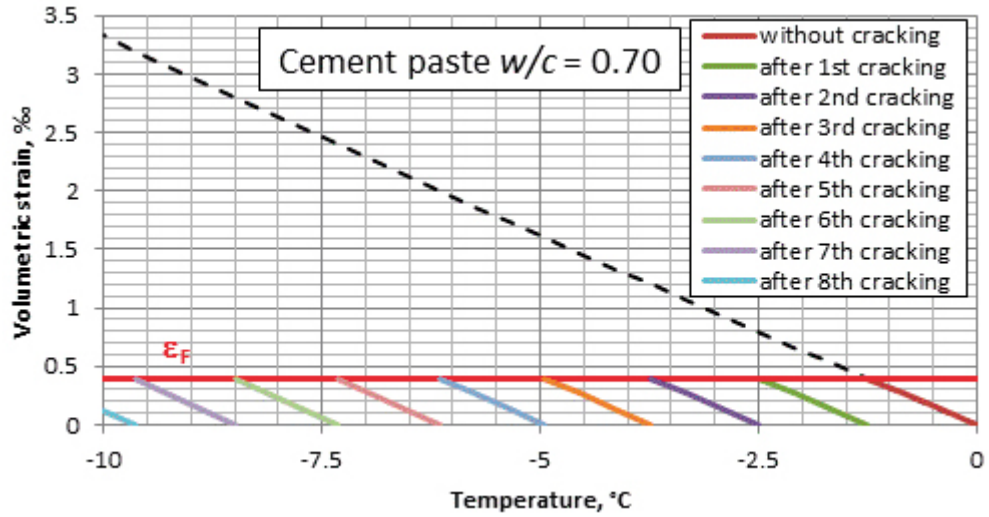

Figure 6-4b. *Possible cracking during freezing in hardened cement paste in the 1 BMA concrete with w/c 0.70 (as the lower limit).*

Table 6-1. Possible cracking in hardened cement pastes with w/c 0.44–0.50 (Silo concrete).

Properties of cement paste	Lower	Mean	Upper
w/c	0.5	0.47	0.44
Compresive strength f_{cu}, MPa	43	48	55
Cement content, kg/m^3 (fresh paste)	1,223	1,270	1,320
Dry paste, kg/m^3 (hardened paste)	1,505	1,562	1,624
Porosity of hardened paste ϕ_0	0.401	0.378	0.353
Capillary porosity of hardened paste ϕ_{cap}	0.168	0.136	0.102
Evaporable water w_e, kg/m^3 (hardened paste)	401	378	353
Elastic modulus of concrete E_c, GPa	25.7	26.6	27.4
Elastic modulus of paste E_p, GPa [Eq. 6-10]	10.2	11	11.8
Biot coefficient *b* [Eq. 6-8]	0.572	0.549	0.522
Cracking during freezing			
1st cracking	–1.8°C	–2.0°C	–2.3°C
Number of cracking at –5°C	2	2	2
Number of cracking at –10°C	5	5	4

Table 6-2. Possible cracking in hardened cement pastes with w/c 0.55–0.70 (1 BMA concrete).

Properties of cement paste	Lower	Mean	Upper
w/c	0.7	0.62	0.55
Compresive strength f_{cu}, MPa	35	40	45
Cement content, kg/m^3 (fresh paste)	983	1,067	1,153
Dry paste, kg/m^3 (hardened paste)	1,209	1,312	1,418
Porosity of hardened paste ϕ_0	0.518	0.477	0.435
Capillary porosity of hardened paste ϕ_{cap}	0.331	0.274	0.216
Evaporable water w_e, kg/m^3 (hardened paste)	518	477	435
Elastic modulus of concrete E_c, GPa	24.1	25.1	26
Elastic modulus of paste E_p, GPa [Eq. 6-10]	8.8	9.6	10.4
Biot coefficient *b* [Eq. 6-8]	0.682	0.646	0.606
Cracking during freezing			
1st cracking	–1.3°C	–1.5°C	–1.7°C
Number of cracking at –5°C	4	3	3
Number of cracking at –10°C	8	7	6

7 Extended calculation

In this section, we will calculate the strains due to liquid overpressure during freezing under different variations. From the previous section it can be seen that the number of cracking at a certain temperature can directly be estimated from the total volumetric strain at that temperature. Therefore, in the following calculation, we only indicate the temperature when the first cracking occurs, and the total volumetric strain and the number of cracking at –5°C and –10°C, respectively.

Case 2: Assuming an increase in the β value in Equation 4-1 by a factor of 2 (implying 200% freezable water when compared with basic case). The results are shown in Figure 7-1. It can be seen that, for the silo concrete, the first cracking may occur at temperature –1.0°C. At –5°C and –10°C the total volumetric strain will be 2.2‰ and 5.0‰, respectively, and the number of cracking will be 5 and 12, respectively. For the 1 BMA concrete, the first cracking may occur at temperature –0.7°C. At –5°C and –10°C the total volumetric strain will be 3.0‰ and 6.6‰, respectively, and the number of cracking will be 7 and 16, respectively.

Case 3: Assuming an increase in the β value in Equation 4-1 by a factor of 3 (implying 300% freezable water when compared with basic case). The results are shown in Figure 7-2. For the silo concrete, the first cracking may occur at temperature –0.6°C. At –5°C and –10°C the total volumetric strain will be 3.6‰ and 8.8‰, respectively, and the number of cracking will be 9 and 21, respectively. For the 1 BMA concrete, the first cracking may occur at temperature –0.5°C. At –5°C and –10°C the total volumetric strain will be 4.7‰ and 11.4‰, respectively, and the number of cracking will be 11 and 28, respectively.

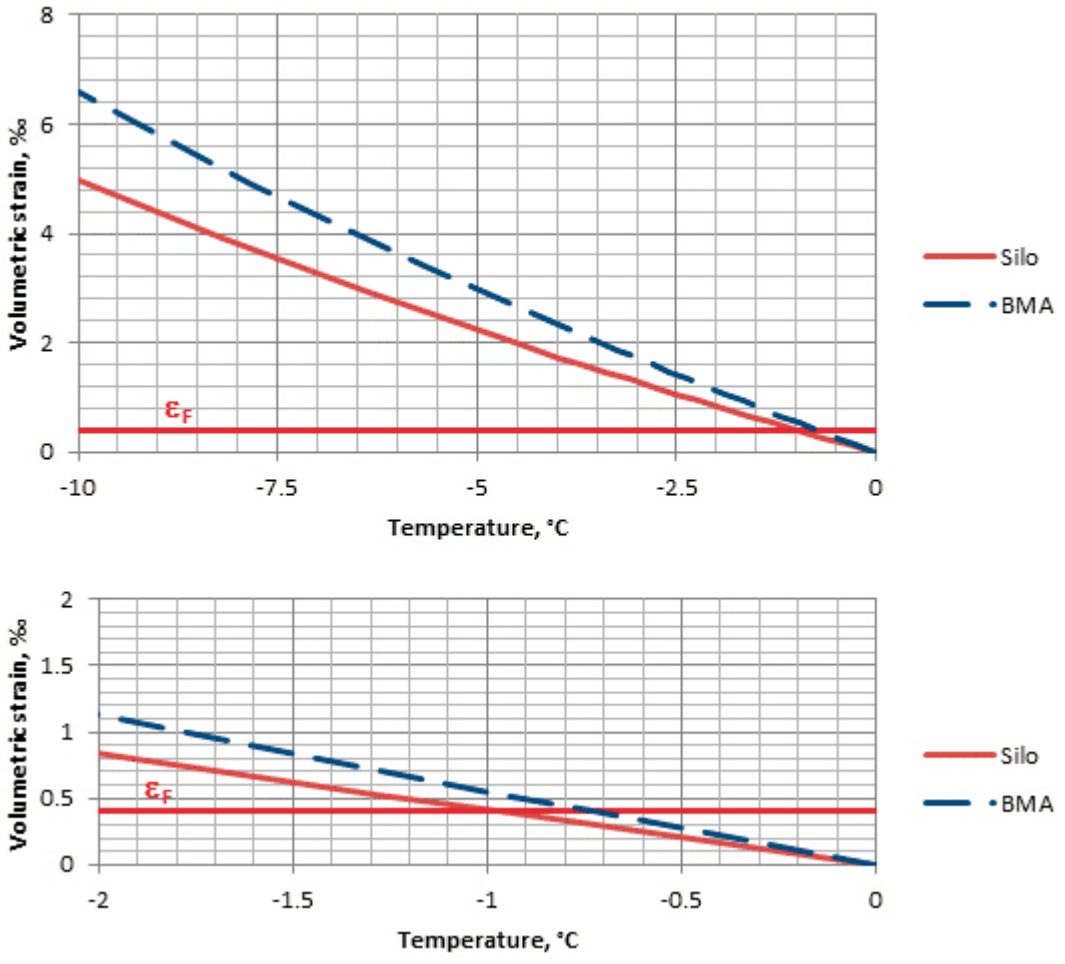

Figure 7-1. *Volumetric strains during freezing in Case 2, with 200% freezable water.*

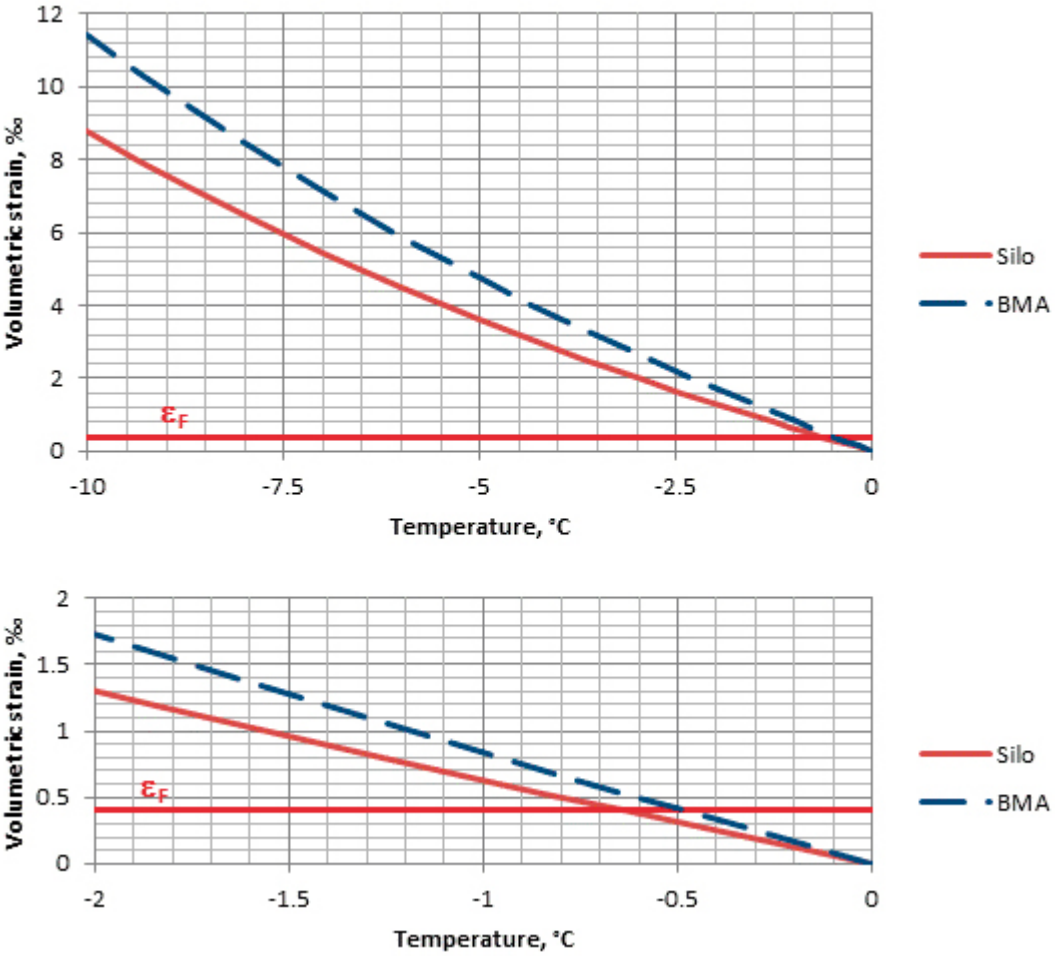

Figure 7-2. *Volumetric strains during freezing in Case 3, with 300% freezable water.*

Case 4: Assuming an increase in the β value in Equation 4-1 by a factor of 4 (implying 400% freezable water when compared with basic case). The results are shown in Figure 7-3. For the silo concrete, the first cracking may occur at temperature –0.5°C. At –5°C and –10°C the total volumetric strain will be 5.2‰ and 14.1‰, respectively, and the number of cracking will be 12 and 35, respectively. For the 1 BMA concrete, the first cracking may occur at temperature –0.4°C. At –5°C and –10°C the total volumetric strain will be 6.8‰ and 18‰, respectively, and the number of cracking will be 16 and 45, respectively.

The calculated results under different cases for the silo and 1 BMA concrete are summarised in Tables 7-1 and 7-2, respectively.

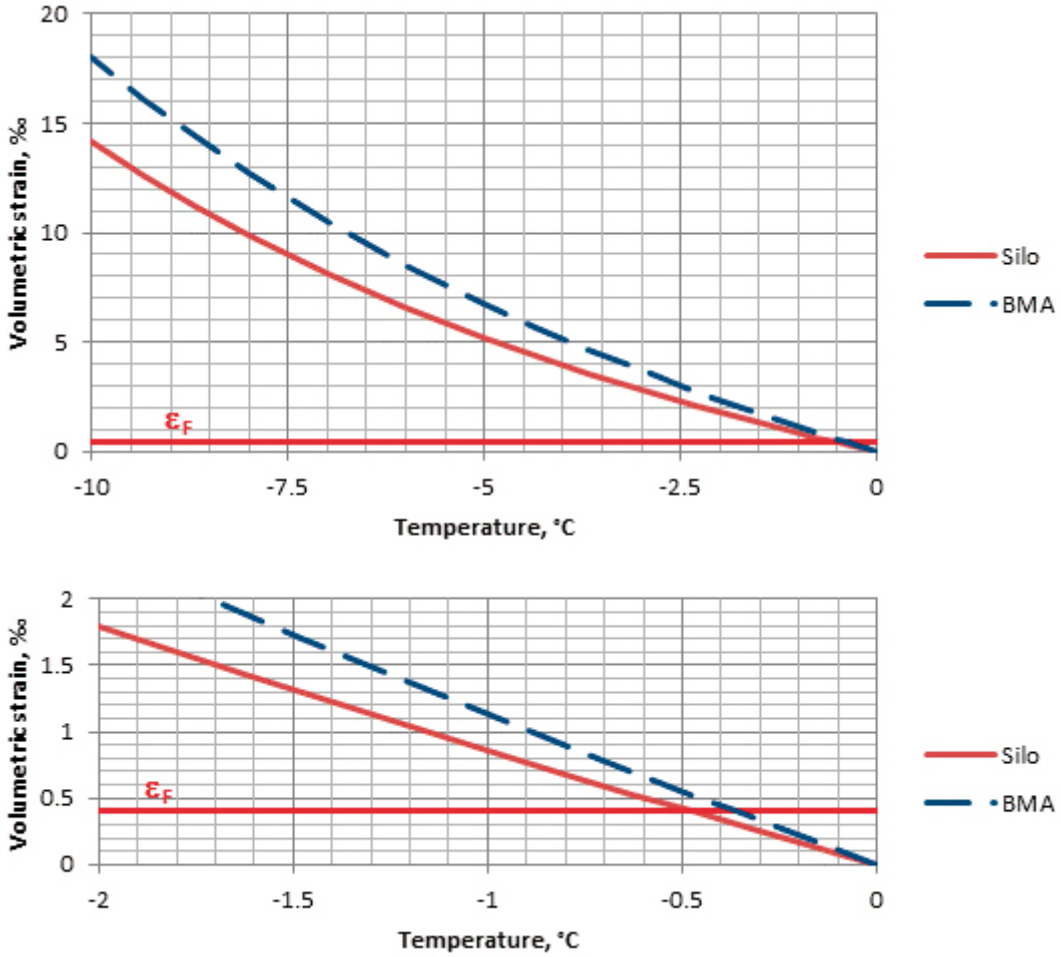

Figure 7-3. *Volumetric strains during freezing in Case 4, with 400% freezable water.*

Table 7-1. Summary of possible cracking in hardened cement pastes w/c 0.47 (Silo concrete).

	Case 1*	Case 2	Case 3	Case 4
1st cracking	–2.0°C ± 0.3°C	–1.0°C	–0.6°C	–0.5°C
Vol. strain at –5°C	1.0‰ ± 0.13‰	2.2‰	3.6‰	5.2‰
Number of cracking	2	5	9	12
Vol. strain at –10°C	2.1‰ ± 0.27‰	5.0‰	8.8‰	14.1‰
Number of cracking	4–5	12	21	35

* Presented as mean ± standard deviation from three calculations (basic, upper and lower limits).

Table 7-2. Summary of possible cracking in hardened cement pastes w/c 0.62 (1 BMA concrete).

	Case 1*	Case 2	Case 3	Case 4
1st cracking	–1.5°C ± 0.2°C	–0.7°C	–0.5°C	–0.4°C
Vol. strain at –5°C	1.4‰ ± 0.20‰	3.0‰	4.7‰	6.8‰
Number of cracking	3–4	7	11	16
Vol. strain at –10°C	2.9‰ ± 0.41‰	6.6‰	8.4‰	18.0‰
Number of cracking	6–8	16	28	45

* Presented as mean ± standard deviation from three calculations (basic, upper and lower limits).

It should be noticed that Cases 3 and 4 are very unlikely and require that the pores in the hardened cement paste become very coarse while the total pore volume is kept unchanged. This means that the cement hydrates are not as what we know today.

8 Discussion of consequences

8.1 About cracking

As mentioned in the beginning of Chapter 6, in the calculation the criterion of 0.4‰ of volumetric strain was used for cracking. This means that the linear strain is about 0.13‰, or 0.13 mm per meter of hardened cement paste, which is in a micro-scale. Because the hardened cement paste is surrounded by large particles of aggregate, and concrete itself is reinforced by steel bars, these cracks cannot be concentrated but should be relatively homogeneously distributed in a concrete structure. On the other hand, the pores in the hardened cement paste are not with a mono-size, and local cracking can occur even earlier than this criterion, implying that the frost action induces micro-cracks in the hardened cement paste, especially under the undrained condition, at very slow cooling rate. Therefore, the number of cracking summarised in Tables 7-1 and 7-2 does not necessarily mean the actual number of cracks with a size of wideness 130 μm, but just an indication of equivalent quantity of many micro-cracks with a width less than 130 μm.

8.2 Increase in pore volume due to micro-cracking

From the above calculations it can be seen that, for the silo concrete, if Case 1 holds, there will be about 2 times of cracking at –5°C and 4–5 times of cracking at –10°C, resulting in an increase in pore volume by maximum 2×0.04% = 0.08% and 5×0.04% = 0.2% (by volume of hardened cement paste), respectively. In the worst case (Case 4 at –10°C), the volume of micro-cracks will be about 35×0.04% = 1.4% (by volume of hardened cement paste).

For the 1 BMA concrete, if Case 1 holds, there will be about 3–4 times of cracking at –5°C and 6–8 times of cracking at –10°C, resulting in an increase in pore volume by maximum 4×0.04% = 0.16% and 8×0.04% = 0.32% (by volume of hardened cement paste), respectively. In the worst case (Case 4 at –10°C), the volume of micro-cracks will be about 45×0.04% = 1.8% (by volume of hardened cement paste).

8.3 Effect of micro-cracks on mechanical properties

The compressive strength of concrete is inversely proportional to its porosity. As a simple rule, an increase in air pore volume in concrete by 1% corresponds to a decrease in compressive strength by 6% p. 153 in (Domone and Illston 2010).

In the concrete used for SFR 1, the aggregate volume fraction is about 0.7 for both the silo and 1 BMA concrete. Therefore, the paste volume including entrapped air and ITZ is about 0.3 m^3 per m^3 concrete. An increase of pore volume in cement paste by 0.08%, 0.2% and 1.4% in the paste of the silo concrete, and 0.16%, 0.32% and 1.8% in the paste of the 1 BMA concrete as discussed in Section 8.2, can be converted to an increase of pore volume in the silo concrete by 0.024%, 0.06% and 0.42%, and in the 1 BMA concrete by 0.036%, 0.096% and 0.54%. This may decrease the compressive strength of the silo concrete by 0.14%, 0.36% and maximum 2.5%, and that of the 1 BMA concrete by 0.22%, 0.58% and maximum 3.2% respectively. This is less than a standard deviation in concrete production. This estimation is, however, based on the air pore volume. For the volume of micro-cracks the reduction in compressive strength may be larger. According to Jacobsen et al. (1999) a linear dilation of 0.18% (corresponding to a volumetric dilation of 0.54%) resulted in a reduction of compressive strength of concrete with w/c 0.50 by 18.6%. Comparing this reduction with the above estimation, it increased by a factor of about 6. Therefore, it is reasonable to conclude that, after one cycle of freezing-thawing at temperature –5°C and –10°C, the compressive strength of the silo concrete may in normal case (Case 1) be reduced by 0.9% and 2.2%, respectively, and in the worst case (Case 4 at –10°C) by 15.1%, while the compressive strength of the 1 BMA concrete may in normal case (Case 1) be reduced by 1.3% and 3.5%, respectively, and in the worst case (Case 4 at –10°C) by 19.4%. It should be noticed that Case 3 and 4 requires such large changes in pore structure, that such extrapolation is not reliable. Nothing can be said about the compressive strength for these cases. As a conclusion, the change in compressive strength is in normal cases in a range of standard deviation of concrete products.

The tensile strength may, however, be reduced significantly due to the formation of micro-cracks. According to limited experimental data reported by Tang and Petersson (2002), the reduction in flexural strength due to freezing-thawing dilation (excluding the effect of freezing-thawing cycles) may be expressed by the following equation:

$$\Delta f = 1.2\sqrt{\varepsilon_x} \qquad (8\text{-}1)$$

where ε_x is the linear dilation of a concrete specimen after freezing-thawing.

For the silo concrete, the pore volume increases in the silo concrete by 0.024% and 0.06% in Case 1 and 0.42% in the worst case (Case 4 at –10°C) correspond to a linear dilation of 0.008%, 0.02% and 0.14%, resulting in a reduction in flexural or tensile strength by 11%, 17% and 45%, respectively.

For the 1 BMA concrete, the pore volume increases in the silo concrete by 0.036% and 0.096% in Case 1 and 0.54% in the worst case (Case 4 at –10°C) correspond to a linear dilation of 0.008%, 0.02% and 0.14%, resulting in a reduction in flexural or tensile strength by 13%, 22% and 51%, respectively.

Depending on the safety factor in the structural design of the reinforced concrete, the reduction in tensile strength by about 20% in normal cases may not result in significant cracking in the structure. However the reduction in tensile strength by about 50% in the extreme case may result in significant cracking in the structure. The relationship between the minimum area of reinforcing steel and the mean value of the tensile strength of the concrete has been given in EC 2, (SS-EN 1992-1-1:2005) (Section 7.3.2). Because both the concrete silo and 1 BMA are filled with grout after filling of the radioactive waste, it is hardly possible to lead a structural collapse due to the reduction in tensile strength of concrete even by 50%, unless the steel reinforcement in the reinforced concrete structure is designed with significantly less amount of steel bars and there exists large unfilled volume under the concrete roof. The detailed deflection control of reinforced concrete has been described in EC 2, (SS-EN 1992-1-1:2005) (Section 7.4).

8.4 Effect of micro-cracking on hydraulic conductivity

It is reasonable to count these micro-cracks as large capillary pores with size of ≤ 0.13 mm (linear strain ≈ 1/3 of volumetric strain). For the cement paste with *w/c* 0.47 ± 0.03 in the silo concrete and *w/c* 0.62 ± 0.07 in the 1 BMA concrete, the initial total (gel + capillary) porosity (see Tables 6-1 and 6-2) is 0.377 ± 0.024 and 0.477 ± 0.042, respectively, and the capillary porosity (also see Tables 6-1 and 6-2) is about 0.135 ± 0.033 and 0.274 ± 0.058, respectively, according to Equations 5-15 and 5-16. Under the assumption that the hydraulic conductivity (permeability) of concrete is proportional to its capillary porosity, an increase in capillary pore volume by 0.08% to 0.2% in the paste of the silo concrete is equal to an increase in capillary porosity by 0.0008/0.135 = 0.006 and 0.002/0.135 = 0.015, implying an increase in the hydraulic conductivity of such a type of concrete by 0.6% and 1.5% after one cycle of freezing-thawing at temperature –5°C and –10°C, respectively. Similarly, an increase in capillary pore volume by 0.16% to 0.32% in the paste of the 1 BMA concrete is equal to an increase in capillary porosity by 0.0016/0.274 = 0.006 and 0.0032/0.274 = 0.012, implying an increase in the hydraulic conductivity of such a type of concrete by 0.6% and 1.2% after one cycle of freezing-thawing at temperature –5°C and –10°C, respectively. These decreases are insignificant.

In the worst case (Case 4 at –10°C), although very unlikely, the volume of micro-cracks in the paste of the silo and the 1 BMA concrete will be about 1.4% and 1.8%, respectively, corresponding to an increase in capillary porosity by 0.014/0.135 = 0.1 and 0.018/0.274 = 0.07, respectively. This means that in the worst case the hydraulic conductivity may increase by about 10% in the silo concrete and 7% in the 1 BMA concrete after one cycle of freezing-thawing. This increase in hydraulic conductivity is still very small, especially when taking into account the measurement uncertainty involved in the permeability tests.

8.5 Some thoughts about water saturation

As mentioned earlier in Chapter 5, the silo concrete walls are surrounded by saturated bentonite clay or saturated sand/bentonite mixture and the 1 BMA concrete walls are surrounded by saturated gravel filler. The surrounding water will freeze earlier than the pore water in both the bentonite clay layer and the concrete. Since the chemical potential of ice is lower than that of the pore water, the ice in the surrounding materials will attract water from the bentonite clay layer and the concrete. This attracted exceed water may flow away downwards before the bottom layer freezes. Thus the degree of saturation of the concrete will be reduced, which will lead to reduced internal damage of the concrete due to freeze-thaw action.

If concrete is partially saturated, the outer layer of concrete will have a high degree of saturation due to the mechanisms mentioned:

- Increased salinity in the surroundings and the outer surface, and
- Ice formation in the surrounding materials (groundwater or bentonite layer).

Serious damage from freeze-thaw exposure of concrete normally requires several freeze-thaw cycles, during which formation, and melting, of micro ice lenses lead to extra water uptake, even in specimens which have been saturated by capillary suction. Thus, during the few cycles expected during the coming periods with permafrost, only a small amount of extra water will be taken up (Bager 2010).

9 Concluding remarks

Based on the model used in this study, if the concrete for SFR 1 is fully saturated under the permafrost period, the following conclusions can be drawn:

- The effect of ionic concentration (salinity) in the pore solution on the depression of freezing point is insignificant due to insufficient high concentration, especially after long-term leaching, although there may be a temporary high concentration period due to the permafrost passage.
- Under the normal case, the first cracking may occur when temperature decreases to the range of –1.8°C to –2.3°C for the silo concrete and –1.3°C to –1.7°C for the 1 BMA concrete.
- For the silo concrete under the normal case, it may occur 2 times of cracking when temperature decreases to –5°C and 4–5 times of cracking when temperature decreases to –10°C.
- For the 1 BMA concrete under the normal case, it may occur 3–4 times of cracking when temperature decreases to –5°C and 6–8 times of cracking when temperature decreases to –10°C.
- Under the worst case (Case 4 at –10°C), although very unlikely, the first cracking may occur at –0.5°C for the silo concrete and –0.4°C for the 1 BMA concrete. The maximum volumetric strain will be 1.4% by volume of hardened cement paste or 0.42% by volume of the silo concrete, and 1.8% by volume of hardened cement paste or 0.54% by volume of the 1 BMA concrete.
- After one cycle of freezing-thawing at temperature –5°C and –10°C, the compressive strength of the silo concrete may in normal case be reduced by 1% and 2%, respectively, and in the worst case by 15%. The compressive strength of the 1 BMA concrete may in normal case be reduced by 1% and 4%, respectively, and in the worst case by 19%.
- After one cycle of freezing-thawing at temperature –5°C and –10°C, the tensile strength of the silo concrete may in normal case be reduced by 11% and 17%, respectively, and in the worst case by 45%. The tensile strength of the 1 BMA concrete may in normal case be reduced by 13% and 22%, respectively, and in the worst case by 51%.
- After one cycle of freezing-thawing at temperature –5°C and –10°C, the hydraulic conductivity of both the silo and the 1 BMA concrete may in normal case be increased by not more than 2%, and in the worst case by not more than 10%.
- It is hardly possible to lead a structural collapse due to the reduction in tensile strength in both the silo and the 1 BMA concrete containers filled inside with grout after filling of nuclear waste, unless the steel reinforcement in the reinforced concrete structure is designed with significantly less amount of steel bars and there exists large unfilled volume under the concrete roof.

If the concrete is not fully saturated due to the reasons as discussed in Section 8.5, it is foreseen that only minor frost damage will occur in the outer concrete layer in the concrete structures for SFR 1, under the condition that the expected crack formation in the rock above the SFR 1 structures appears.

The above conclusions are based on the concrete with fully hydrated cement, but without taking into account the ageing effect after long-term (thousands years) exposure. Following further research is needed in order to secure the above conclusions:

- Quantitative dilation of fully saturated hardened cement paste after one cycle of freezing-thawing.
- Quantitative relationship between mechanical properties of fully saturated hardened cement paste and concrete specimens after freezing-thawing cycles.
- Quantitative relationship between transport properties of fully saturated hardened cement paste and concrete specimens after freezing-thawing cycles.

It should be noticed that the measurement of hydraulic conductivity (water permeability) of concrete with such a low *w/c* ratio (0.44–0.50) is not an easy task. It is suggested that the ionic diffusion test and the rapid chloride migration test may be used to indirectly evaluate the hydraulic conductivity of cement paste and concrete in order to establish the quantitative relationship between transport properties of fully saturated hardened cement paste and concrete specimens after freezing-thawing cycles.

References

SKB's (Svensk Kärnbränslehantering AB) publications can be found at www.skb.se/publications.

Bager D H, 2010. Qualitative description of the micro ice body freeze-thaw damage mechanism in concrete. NCR Workshop Proceeding No. 9: Nordic miniseminar : Freeze-thaw testing of concrete – Input to revision of CEN test methods, Vedbæk, Denmark, 4–5 March, 2010.

Bager D H, Hansen T B, 1999. Influence of water-binding on the ice formation and freeze/thaw damage in cement paste and concrete. NCR Workshop Proceeding No.1: Nordic miniseminar: Water in cement paste and concrete, hydration and pore structure, Skagen, Denmark, 7–8 October 1999.

Coussy O, Monteiro P J M, 2008. Poroelastic model for concrete exposed to freezing temperatures. Cement and Concrete Research 38, 40–48.

Coussy O, Monteiro P J M, 2009. Errata to "Poroelastic model for concrete exposed to freezing temperatures [Cement and Concrete Research 38, 40–48]". Cement and Concrete Research 39, 371–372.

Domone P L J, Illston J M (eds), 2010. Construction materials: their nature and behaviour. 4th ed. Milton Park, Abingdon, Oxon: Spon Press.

Emborg M, Jonassson J-E, Knutsson S, 2007. Långtidsstabilitet till följd av frysning och tining av betong och bentonit vid förvaring av låg-och medelaktivt kärnavfall i SFR 1. SKB R-07-60, Svensk Kärnbränslehantering AB. (In Swedish.)

Hashin Z, Shtrikman S, 1963. A variational approach to the theory of the elastic behaviour of multiphase materials. Journal of the Mechanics and Physics of Solids 11, 127–140.

Höglund L-O, 2001. Project SAFE. Modelling of long-term concrete degradation processes in the Swedish SFR 1 repository. SKB R-01-08, Svensk Kärnbränslehantering AB.

Jacobsen S, Bager D H, Kukko H, Tang L, Nordström K, 1999. Measurement of internal cracking as dilation in the SS 13 72 44 frost test. Nordtest project 1389-98. Oslo: Norges byggforskningsinstitutt NBI.

Jacobsen S, Melandsø F, Nguyen H T, 2004. Flow calculation and thermodynamics in wet frost exposure of cement based materials. In Weiss J, Kovler K, Marchand J, Mindess S (eds). Proceedings of International RILEM Symposium on Concrete Science and Engineering: a tribute to Arnon Bentur, North Western University, Evanston, Illinois, 22–24 March 2004.

Näslund J-O, 2006. Climate and climate-related issues for the safety assessment SR-Can. SKB TR-06-23, Svensk Kärnbränslehantering AB.

Sellevold E J, Bager D H, 1980. Low temperature calorimetry as a pore structure probe. In Proceedings of the 7th International Congress on the Chemistry of Cements, Paris, July 1980. Vol 4. Paris : Éditions Septima.

SS-EN 1992-1-1:2005. Eurocode 2: Design of concrete structures – Part 1-1: General rules and rules for buildings. Stockholm: Swedish Standards Institute.

Tang L, Petersson P-E, 2002. Water uptake, dilation and internal deterioration of concrete due to freezing-and-thawing. In Setzer M J, Auberg R, Keck H-J (eds). Frost resistance of concrete: proceedings of the International RILEM Workshop on Frost Resistance of Concrete, Essen, Germany 18–19 April 2002, Cachan: RILEM Publications, 287–294.

Vidstrand P, Rhén I, 2011. On the role of model depth and hydraulic properties for groundwater flow modelling during glacial climate conditions. SKB R-10-74, Svensk Kärnbränslehantering AB.